Journal of Power Sources 196 (2011) 4735–4740

Contents lists available at ScienceDirect

Journal of Power Sources

journal homepage: www.elsevier.com/locate/jpowsour

Mesoporous polyaniline/TiO_2 microspheres with core–shell structure as anode materials for lithium ion battery

C. Lai, H.Z. Zhang, G.R. Li, X.P. Gao*

Institute of New Energy Material Chemistry, Tianjin Key Laboratory of Metal and Molecule Based Material Chemistry, Nankai University, Tianjin 300071, China

ARTICLE INFO

Article history:
Received 7 November 2010
Received in revised form 7 January 2011
Accepted 20 January 2011
Available online 28 January 2011

Keywords:
Lithium-ion batteries
Titanium dioxide
Polyaniline
Mesoporous
Core–shell

ABSTRACT

Mesoporous polyaniline/anatase TiO_2 composite microspheres with the core–shell structure for lithium-ion battery applications are prepared via a facile hydrothermal route. The structure of as-prepared sample is characterized by electron microscopy (TEM), and scanning electron microscopy (SEM), X-ray diffraction (XRD), and Brunauer–Emmett–Teller (BET) surface area. It is suggested that the formation of the core–shell structure can be designated as a two-step assembly process induced by the polymerization of the aniline. The electrochemical tests demonstrate that the discharge capacity of the as-prepared polyaniline/anatase TiO_2 microspheres can be stably retained at 157.1 mAh g^{-1} after 50th cycle at the high current density of 1500 mA g^{-1}. The high rate performance of the as-prepared sample at various current densities from 200 to 2000 mA g^{-1} is also investigated. The discharge capacity of 123.9 mAh g^{-1} can be obtained at the high current density of 2000 mA g^{-1}, which is about 73.4% of that at the low current density of 200 mA g^{-1} upon cycling, indicating that the as-prepared sample can endure great changes of various current densities to retain a good stability due to the core shell mesoporous structure.

1. Introduction

Rechargeable lithium-ion batteries play an important role in portable electronic devices, electric vehicles (EVs) and hybrid electric vehicles (HEVs). Safety is one of primary concerns in such applications of lithium-ion batteries (LIBs), especially for automobile applications [1]. Among those safe alternatives for graphite anode, titanium compounds, such as TiO_2 and $Li_4Ti_5O_{12}$, are of particular interest due to a relatively high operation potential around 1.5 V (vs. Li^+/Li) to avoid the deposition of metallic lithium and the decomposition of organic electrolyte during the electrochemical discharge/charge process [2–5]. Meanwhile, in order to enhance the power density of LIBs, electrode must possess an excellent high rate capability based on nanocrystalline active materials due to short diffusion lengths for electrons and lithium ions, and as well as increased reaction active sites [1,6]. In recent decades, the introduction of nanocrystallites into the electrode active materials for LIBs has attracted great interest. Furthermore, to meet requirements in the practical electrode production, micron-sized spherical materials should be more favorable based on their advantages of excellent flowability, easily loading and high packing density [2,7,8]. In such microspherical active materials, a core–shell hierarchical architecture is also demonstrated to be superior to provide a buffer layer to accommodate the volume expansion of the electrode during the discharge and charge processes [9–13]. Moreover, mesoporous TiO_2 materials with the high packing density is demonstrated recently to present a superior electrochemical lithium storage performance as compared with commercial TiO_2 nanoparticles [2]. Therefore, it is necessary to prepare microspheres assembled with nanocrystallites to form three-dimensional channels with mesoporous and core–shell hierarchical architecture.

In this work, polyaniline/anatase TiO_2 micropsheres with core–shell structure are prepared via a facile one-step hydrothermal route, herein TiO_2 nanocrystallites present an excellent high rate capability, and the amorphous polymer layer on TiO_2 nanocrystallites can provide a buffer layer to ensure the cycle stability [6,14,15]. Thus, the excellent performance can be expected for the as-prepared polyaniline/anatase TiO_2 microspheres.

2. Experimental

2.1. Preparation and characterization

Titanium precursor solution was prepared by dissolving $TiOSO_4{\cdot}2H_2O$ (chemical, 6.26 g) in H_2O (120 mL). In a typical process for synthesizing polyaniline/TiO_2 microspheres with core–shell structure, aniline (analytical, 0.1 mL) was dissolved in ethanol (25 mL), and then added into $TiOSO_4$ solution (15 mL) with $FeCl_3{\cdot}6H_2O$ (analytical, 0.3 g) under stirring. After the mixed solution turned clear, the resultant solution was transferred into

* Corresponding author. Tel.: +86 22 23500876; fax: +86 22 23500876.
E-mail address: xpgao@nankai.edu.cn (X.P. Gao).

0378-7753/$ – see front matter © 2011 Elsevier B.V. All rights reserved.
doi:10.1016/j.jpowsour.2011.01.077

a Teflon-lined autoclave (55 mL) and treated at 140 °C for 6 h. The obtained precipitates were washed with distilled water and ethanol, and dried under vacuum at 60 °C. To investigate the formation mechanisms of composite microspheres, a synthesis reaction without $FeCl_3 \cdot 6H_2O$ as catalyst was also carried out under the same condition to obtain blank sample (designated as blank TiO_2). In order to obtain TiO_2 microspheres, the obtained polyaniline/TiO_2 composite microspheres was calcined at 500 °C for 3 h with a rate of 2 K min^{-1} in a muffle furnace in air.

The as-prepared sample was characterized by Fourier transform infrared (FTIR, BIO-RAD FTS6000) spectra, X-ray diffraction (XRD, RIGAKU D/max-2500), Brunauer–Emmett–Teller (BET, ASAP 2020) measurements, scanning electron microscopy (SEM, HITACHI S-4800), and transmission electron microscopy (TEM, FEI Tecnai 20).

2.2. Electrochemical measurements

The working electrode was prepared by compressing a mixture of active materials, acetylene black, and binder (poly(tetrafluoroethylene, PTFE) in a weight ratio of 80:15:5. The weight of working electrodes is about 3 mg. Lithium metal was used as the counter and reference electrodes. The electrolyte was LiPF6 (1 M) dissolved in a mixture of ethylene carbonate (EC), ethyl methyl carbonate (EMC) and dimethyl carbonate (DMC) with a volume ratio of 1:1:1. The galvanostatic method at the different charge/discharge current densities of 200, 500, 1000, 1500 and 2000 mA g^{-1} was employed to measure the electrochemical capacity and cycle life of the working electrode at room temperature using a LAND-CT2001A instrument. The cut-off potentials for charge and discharge were set at 2.5 and 1.0 V (vs. Li^+/Li), respectively. The cyclic voltammetery (CV) experiment was conducted using a CHI 600A potentiostat at various scan rates. The electrochemical impedance spectra (EIS) were recorded in the frequency range from 100 kHz to 10 mHz at 5 mV of the amplitude of perturbation by using an IM6e electrochemical workstation (ZAHNER). All electrochemical measurements were carried out at room temperature.

3. Results and discussion

Polyaniline/TiO_2 core–shell composite microspheres can be obtained just by hydrothermal treating the mixing solution of $TiOSO_4$ and aniline with Fe^{3+} as catalyst. The formation of anatase TiO_2 and polyaniline can be confirmed from FTIR spectra and XRD patterns shown in Fig. 1. The FTIR spectra of the core–shell composite microspheres, as shown in Fig. 1a, presents four characteristic peaks at 1141.8 cm^{-1} (C–H plane-bending vibration), 1307.7 cm^{-1} (C–N stretching vibration), 1504.4 cm^{-1} (benzenoid ring stretching mode), and 1577.7 cm^{-1} (quinoid ring stretching mode), respectively, for identifying the existence of polyaniline in the nanocomposites [16–21]. For the blank TiO_2, the characteristic peaks of polyaniline cannot be observed, and the bands appearing between 1700 and 1000 cm^{-1} can be attributed to the TiO_2 and trace aniline adsorbed. The difference between the core–shell composite and the blank sample further confirmed the generation of polyaniline via an oxidative polymerization process. It is worth noted that there is the obvious band appearing around 1050 cm^{-1} for both the as-prepared polyaniline/anatase TiO_2 microspheres and the blank TiO_2, which is designated as the split peak of C–H plane-bending vibration, and this indicates the strong interaction between nanocrystalline TiO_2 and aniline monomer or polyaniline [18]. XRD patterns of the as-prepared polyaniline/anatase TiO_2 microspheres and the blank TiO_2 are given in Fig. 1b. All the peaks can be indexed as the anatase phase, and there is no difference between the core–shell composite and the blank sample. However, the polyaniline in the core–shell composite microspheres is not detected due to its amorphous state [21]. By calculating from Scherrer's formula, the crystallite sizes for the core–shell composite and the blank TiO_2 are 13.0 and 13.2 nm. Different from previous report [15], it is obvious that the growth of nanostructured TiO_2 is not restricted by the polyaniline in the core–shell composite microspheres, indicating that the generation of nanocrystalline TiO_2 is a faster process. Thus, it is believed that the generation of nanocrystalline TiO_2 and the polymerization of aniline are

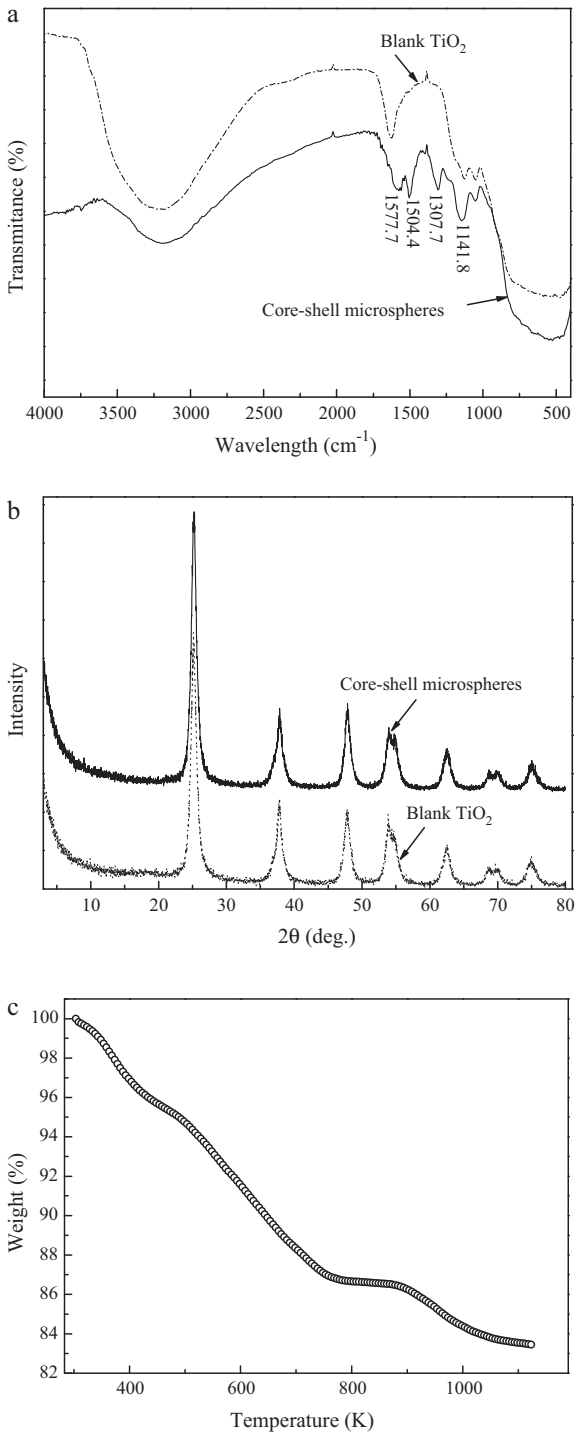

Fig. 1. (a) FTIR spectra and (b) XRD patterns of the as-prepared polyaniline/anatase TiO_2 microspheres and the blank TiO_2 (dashed line); (c) TGA plot of the as-prepared polyaniline/anatase TiO_2 microspheres.

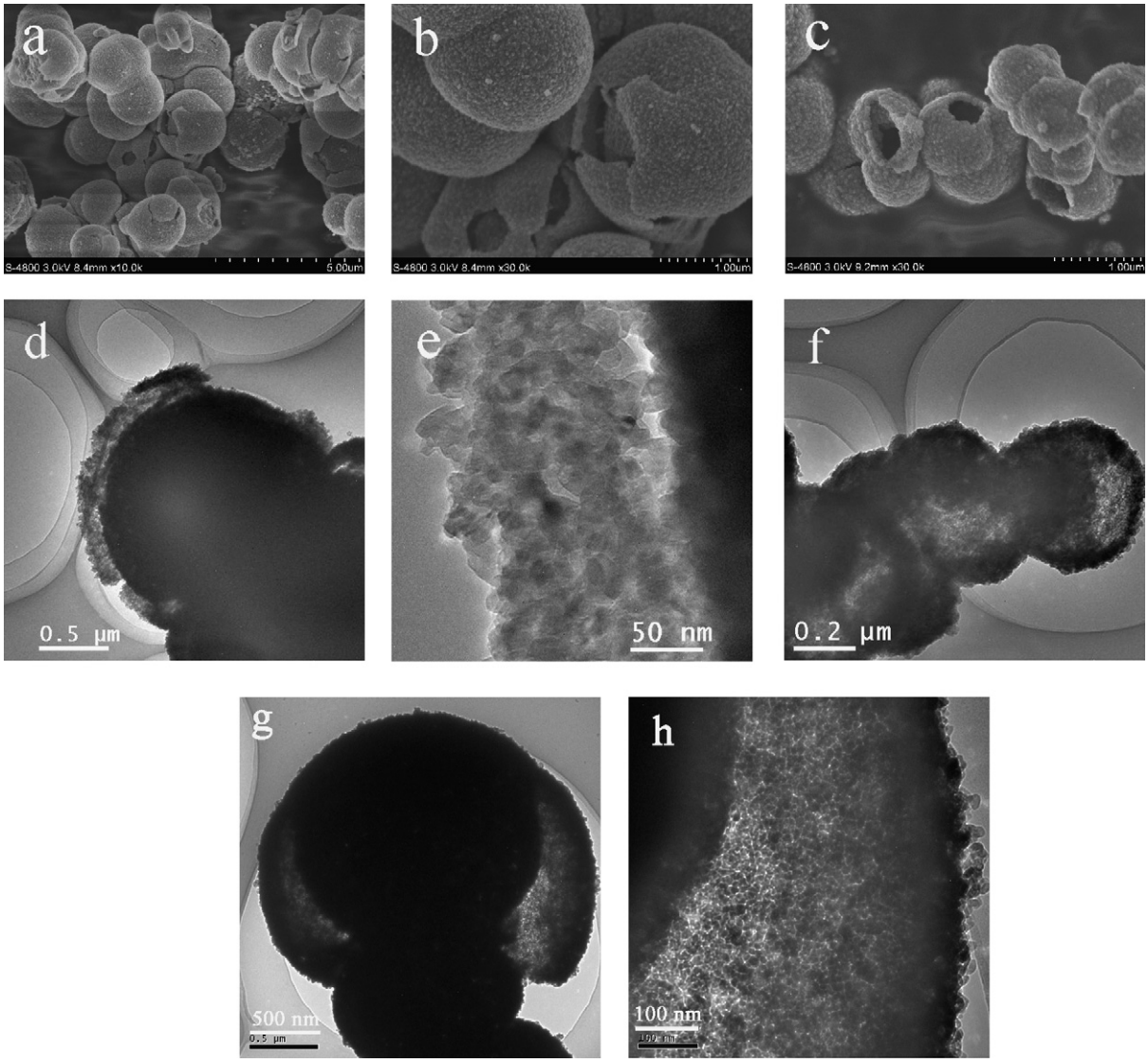

Fig. 2. SEM and TEM images of the as-prepared polyaniline/anatase TiO_2 microspheres (a, b, d and e), the blank TiO_2 (c and f) and the TiO_2 microspheres (g and h).

multistep processes and the formation of the core–shell composite microspheres may be a two-step assembly process. Based on the TGA analysis of the as-prepared composite microspheres, the amount of polyaniline in the composite is approximately calculated to be about 9 wt%, as the decomposition temperature of polyaniline in air mainly ranges from 500 K to 800 K [22].

To reveal the microstructure of the as-prepared microspheres and the blank TiO_2, representative SEM and TEM images are shown in Fig. 2. From SEM images, the as-prepared microspheres with typical size of about 1–2 μm are spherical aggregates assembled with primary nanocrystallites (Fig. 2a and b). Moreover, the core–shell nature of the as-prepared sample is clearly observed from partially broken microspheres in Fig. 2b. Further insight into the microstructure of polyaniline/anatase TiO_2 microspheres can be seen from TEM images (Fig. 2d and e). It is apparent that the as-prepared sample is fabricated with a clear core–shell hierarchical architecture according to the significant difference between the shell and the dark core region due to the thickness contrast. The measured shell thickness is about 150 nm, assembled with nanocrystallites. After the calcination at 500 °C, the core–shell structure is well-retained for TiO_2 microspheres, and the loose aggregates of nanocrystalline TiO_2 are also can be clearly observed illustrated in Fig. 2g and h. For the blank TiO_2 sample, only the hollow nature can be distinctly verified from SEM and TEM images as shown in Fig. 2c and f. The mesoporous structure, induced by the relatively loose aggregate of titania nanocrystallites, is further characterized by the N_2 adsorption–desorption isotherms with the corresponding pore size distribution as given in Fig. 3. The type-IV isotherm with a clear capillary condensation step of the as-prepared sample indicates the presence of mesoporous structure [23,24]. It is also demonstrated from the desorption branches of the isotherm that the as-prepared polyaniline/TiO_2 microspheres have well-defined mesopores centered at 4.5 nm, and the large specific surface area of about 187 $m^2\,g^{-1}$ is obtained for the polyaniline/TiO_2 microspheres. Obviously, such mesoporous microspheres with the core–shell hierarchical architecture, assembled with TiO_2 nanocrystallites, are beneficial to the fast transport of solvated electrolyte and lithium ions throughout electrode materials.

As mentioned above, the polymerization of aniline and the generation of nanocrystalline TiO_2 are the interrupted two-step process. It should be emphasized here that there are strong interactions between the aniline and nanocrystalline TiO_2, and thus the producing of a solid core may be driven by the he polymerization of the aniline. Accordingly, a schematic representation for the as-prepared samples is given in Fig. 4. As illustrated, nanocrys-

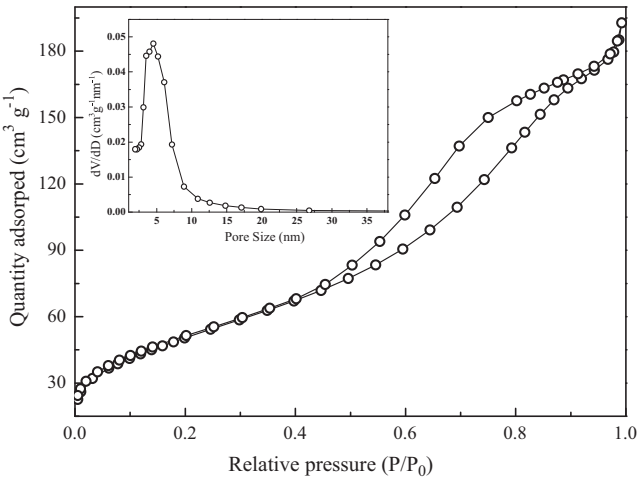

Fig. 3. N_2 adsorption–desorption isotherms and corresponding pore size distribution (inset) of the as-prepared polyaniline/anatase TiO_2 microspheres.

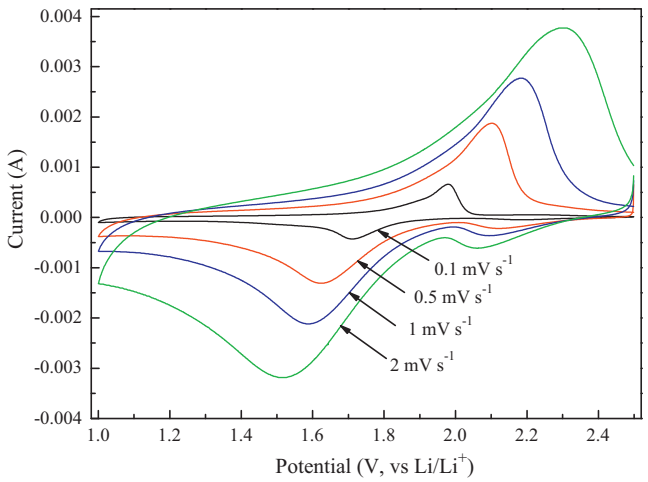

Fig. 5. Cyclic voltammograms of the as-prepared polyaniline/anatase TiO_2 microspheres at different scan rates.

talline TiO_2 is generated gradually in hydrothermal reaction of the $TiOSO_4$ solution, and assembled subsequently to form hollow microspheres. In the reaction system of polyaniline/TiO_2 microspheres, the oxidative polymerization of the aniline with $FeCl_3$ proceed before the generation of the hollow shell, and can produce the solid core with encapsulated anatase TiO_2, thus leading to the formation of the core–shell structure.

For potential battery application, the electrochemical performance of the as-prepared polyaniline/TiO_2 core–shell composite microspheres is investigated. Cyclic voltammograms (CVs) of the as-prepared sample at different scan rates are illustrated in Fig. 5. After the initial two cycles, a pair of redox peaks can be observed at 1.71 and 1.98 V (vs. Li/Li$^+$) at a scan rate of 0.1 mV s^{-1}. These peaks correspond to the insertion and extraction of lithium ion in anatase TiO_2 [25–27], which can still be clearly observed at the high scan rate of 2 mV s^{-1}. Different from previous reports, there is a trace peak appearing around 2.2 V (vs. Li/Li$^+$) during the cathodic process at higher scan rates, which can be attributed to the lithium ion doping in the polyaniline [28,29]. The lithium ion doping process in the polyaniline on the surface may be favorable for the subsequent lithium ion insertion process in the TiO_2 lattices, and this can contribute to the high discharge performance of the core–shell composite microspheres. The discharge–charge curves of the polyaniline/TiO_2 microspheres at the high current density of 1500 mA g^{-1} are presented in Fig. 6a. The initial discharge and charge capacities of the core–shell microspheres are about 241.2 and 190.8 mAh g^{-1}, respectively. The relatively low columbic efficiency in the first cycle is usually attributed to the existence of irreversible Li trapped sites and a trace of adsorbed water, which is a general phenomenon for porous nanomaterials [24–26]. After 50th cycle, the discharge capacity of the polyaniline/TiO_2 microspheres can be stably retained at about 157.1 mAh g^{-1} at the high current density of 1500 mA g^{-1}. In the case of TiO_2 microspheres (Fig. 6b), the initial discharge capacity of TiO_2 microspheres is about 174.1 mAh g^{-1} at the current density of 1500 mA g^{-1}, and the capacity is about 121.2 mAh g^{-1} after 50 cycles. The improved cycle performance of as-prepared composite microspheres can be attributed to the synergistic effect of the polyaniline matrices and nanocrystalline active TiO_2 as discussed above. The introducing of polyaniline is favor to keep the electrode structure stable. Meanwhile, the lower potential polarization of polyaniline/TiO_2 microspheres is observed in the initial charge process as compared with TiO_2 microspheres, in consistent with the analysis of EIS as shown in Fig. 7. Nyquist plots of both the polyaniline/TiO_2 microspheres and TiO_2 microspheres consist of one semicircle at the high frequency region and a straight line at the low frequency region. The semicircle at the high frequency region is related to the charge-transfer process at the electrode–electrolyte interface [30]. Apparently, the charge-transfer resistance (49.97 Ω) of the composite microspheres is much lower than that (80.74 Ω) of TiO_2 microspheres, indicating a faster kinetic process and a good high-rate discharge capability of the composite microspheres.

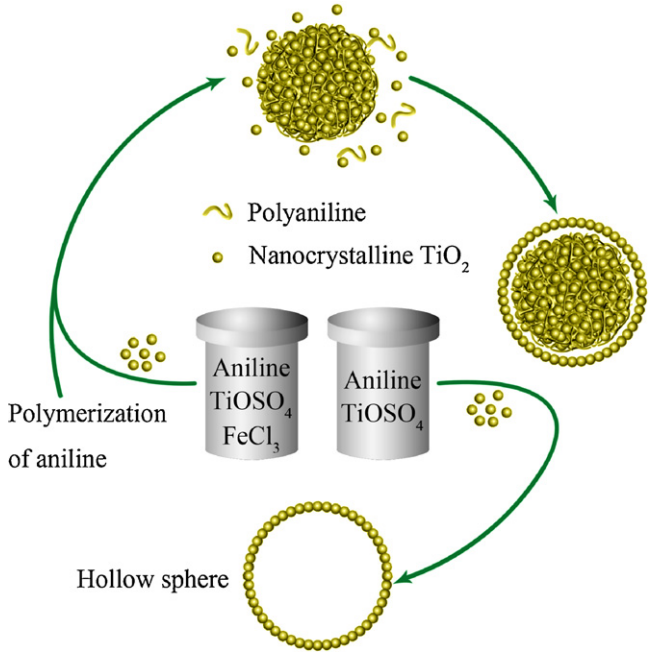

Fig. 4. Schematic representation of the formation of the as-prepared polyaniline/anatase TiO_2 core–shell microspheres and TiO_2 hollow microspheres (blank TiO_2).

To better reveal the high-rate capability and cycle stability of the core–shell microspheres, the variation in discharge capacity with cycles at different current densities is indicated in Fig. 8. The discharge capacity of about 168.7 mAh g^{-1} is obtained after 10th cycle at the low current density of 200 mA g^{-1}. When the current density is increased to 2000 mA g^{-1}, the large capacity is still obtained at 123.9 mAh g^{-1}. More importantly, after 50 cycles at varied current density, the core–shell microspheres still have the discharge capacity of 140.8 mAh g^{-1} at the current density

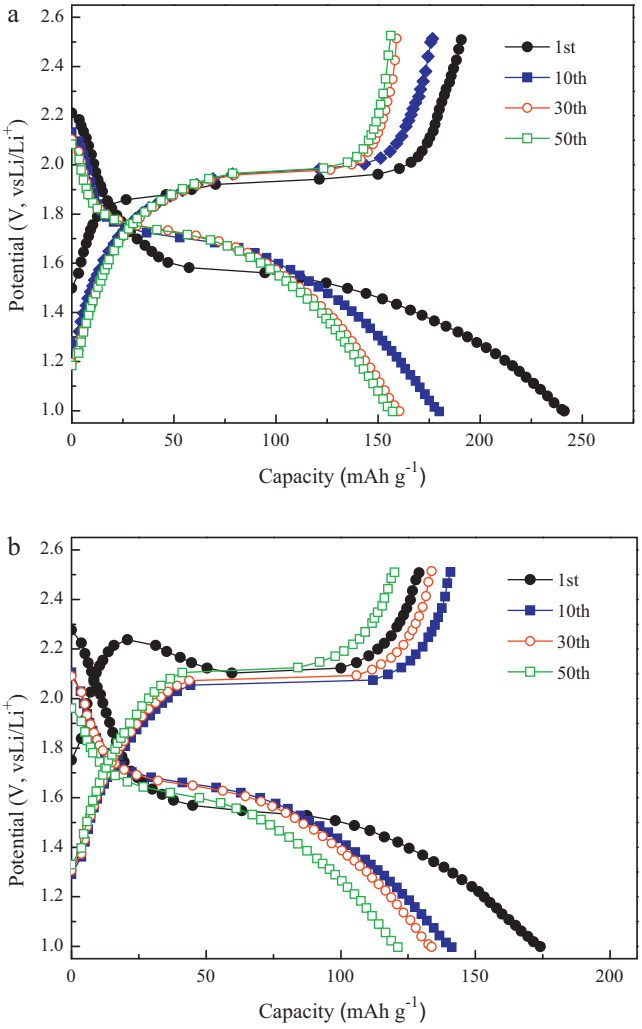

Fig. 6. (a) Discharge–charge curves of the as-prepared polyaniline/anatase TiO_2 microspheres (a) and TiO_2 microspheres (b) at the current density of 1500 mA g^{-1}.

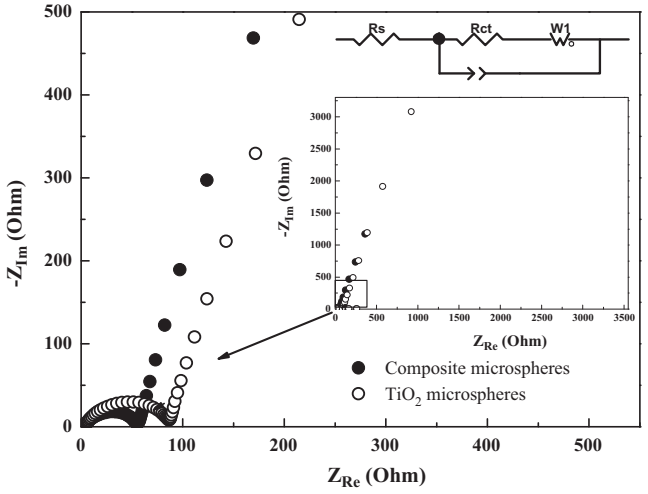

Fig. 7. Nyquist plots of the as-prepared polyaniline/anatase TiO_2 microspheres and TiO_2 microspheres at open-circuit state before cycling.

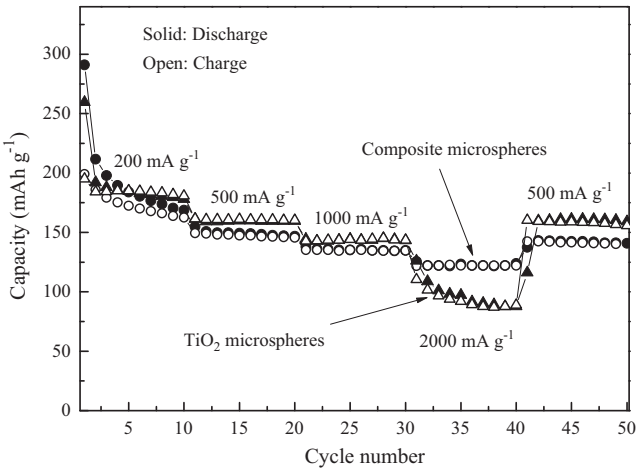

Fig. 8. Cycle performance of the as-prepared polyaniline/anatase TiO_2 microspheres and TiO_2 microspheres at different current densities.

of 500 mA g^{-1}, almost identical to the value in the 20 nd cycle. Therefore, the core–shell microspheres can endure great changes of various low or high current densities to retain good stability upon cycling, and this is a merit for abuse tolerance of lithium-ion batteries with the high power and long cycle life [31]. For the TiO_2 microspheres, a similar discharge performance can be obtained when the current density is below 1000 mA g^{-1}. However, at the large current density of 2000 mA g^{-1}, the discharge capability of the TiO_2 microspheres is poor as compared with that of the composite microspheres. In conclusion, the improved cycle performance and good high-rate performance can be obtained by loading polyanilines into nanocrystalline TiO_2. Furthermore, the as-prepared composite microspheres with developed mesopores has a competing packing density of about 0.708 g cm^{-3}, which is obviously higher than commercial TiO_2 nanopowder (P25) [2].

4. Conclusion

For the application in lithium-ion batteries with the high-rate capability, mesoporous polyaniline/anatase TiO_2 composite microspheres with the core–shell structure are successfully prepared via a facile hydrothermal route. It is suggested that the formation of the core–shell structure involving a two-step assembly process. The as-prepared composite microspheres are favorable for electrode materials with the excellent high rate performance. At the high current density of 1500 mA g^{-1}, the discharge capacity of mesoporous polyaniline/anatase TiO_2 microspheres with the core–shell structure can be stably retained at about 157.1 mAh g^{-1} after 50th cycle. Upon cycling at various current densities, the discharge capacity of 168.7, 146.9, 134.9 and 123.9 mAh g^{-1} is obtained at the current density of 200, 500, 1000 and 2000 mA g^{-1}, respectively. The well retaintion of the discharge capacity indicates that the as-prepared sample can endure great changes of various current densities to retain a good structure and electrochemical stability, and this is a merit for abuse tolerance of lithium-ion batteries with the high power and long cycle life.

Acknowledgments

This work was supported by the 973 Program (2009CB220100), 863 Program (2009AA11A109), MOE Innovation Team (IRT0927), and Fundamental Research Funds for the Central Universities, China.

References

[1] M. Armand, J.M. Tarascon, Nature 451 (2008) 652.
[2] K. Saravanan, K. Ananthanarayanan, P. Balaya, Energy Environ. Sci. 3 (2010) 939.
[3] T. Ohzuku, A. Ueda, N. Yamamoto, J. Electrochem. Soc. 142 (1995) 1431.
[4] P.P. Prosini, R. Mancini, L. Petrucci, V. Contini, P. Villano, Solid State Ionics 144 (2001) 185.
[5] X.P. Gao, H.Y. Zhu, G.L. Pan, S.H. Ye, Y. Lan, F. Wu, D.Y. Song, J. Phys. Chem. B 108 (2004) 2868.
[6] A.S. Arico, P. Bruce, B. Scrosati, J.M. Tarascon, W.V. Schalkwijk, Nat. Mater. 4 (2005) 366.
[7] K. Ohzeki, K. Seino, T. Kumagai, B. Golman, K. Shinohara, Carbon 44 (2006) 578.
[8] J.F. Qian, M. Zhou, Y.L. Cao, X.P. Ai, H.X. Yang, J. Phys. Chem. C 114 (2010) 3477.
[9] K.T. Lee, Y.S. Jung, S.M. Oh, J. Am. Chem. Soc. 125 (2003) 5652.
[10] X.W. Lou, Y. Wang, C.L. Yuan, J.Y. Lee, L.A. Archer, Adv. Mater. 18 (2006) 2325.
[11] Y.K. Sun, S.T. Myung, M.H. Kim, J. Prakash, K. Amine, J. Am. Chem. Soc. 127 (2005) 13411.
[12] D. Deng, M.G. Kim, J.Y. Lee, J. Cho, Energy Environ. Sci. 2 (2009) 818.
[13] J. Liu, W. Li, A. Manthiram, Chem. Commun. 46 (2010) 1437.
[14] Y.G. Wang, W. Wu, L. Cheng, P. He, C.X. Wang, Y.Y. Xia, Adv. Mater. 20 (2008) 2166.
[15] C. Lai, G.R. Li, Y.Y. Dou, X.P. Gao, Electrochim. Acta 55 (2010) 4567.
[16] S.X. Xiong, S.L. Phua, B.S. Dunn, J. Ma, X.H. Lu, Chem. Mater. 22 (2010) 255.
[17] X.W. Li, X.H. Li, N. Dai, G.C. Wang, Z. Wang, J. Power Sources 195 (2010) 5417.
[18] X.W. Li, G.C. Wang, X.X. Li, D.M. Lu, Appl. Surf. Sci. 229 (2004) 395.
[19] D.P. Wang, H.C. Zeng, J. Phys. Chem. C 113 (2009) 8097.
[20] C. Laslau, Z.D. Zujovic, L.J. Zhang, G.A. Bowmaker, J. Travas-Sejdic, Chem. Mater. 21 (2009) 954.
[21] X.Y. Li, D.S. Wang, G.X. Cheng, Q.Z. Luo, J. An, Y.H. Wang, Appl. Catal. B: Environ. 81 (2008) 267.
[22] C.M. Yang, Z. Fang, J. Liu, W.P. Liu, H. Zhou, Thermochim. Acta 352–353 (2000) 159.
[23] Y.M. Cui, L. Liu, B. Li, X.F. Zhou, N.P. Xu, J. Phys. Chem. C 114 (2010) 2434.
[24] H.G. Jung, C.S. Yoon, J. Prakash, Y.K. Sun, J. Phys. Chem. C 113 (2009) 21258.
[25] V. Subramanian, A. Karki, K.I. Gnanasekar, F.P. Eddy, B. Rambabu, J. Power Sources 159 (2006) 186.
[26] J.Z. Chen, L. Yang, Y.F. Tang, J. Power Sources 195 (2010) 6893.
[27] M. Mancini, P. Kubiak, M. Wohlfahrt-Mehrens, R. Marassi, J. Electrochem. Soc. 157 (2010) A164.
[28] S.R. Sivakkumar, D.W. Kim, J. Electrochem. Soc. 154 (2007) A134.
[29] P. Novak, K. Muller, K.S.V. Santhanam, O. Haas, Chem. Rev. 97 (1997) 207.
[30] T. Gao, H. Fjeld, H. Fjellvag, T. Norby, P. Norby, Energy Environ. Sci. 2 (2009) 517.
[31] H. Zhang, X.P. Gao, G.R. Li, T.Y. Yan, H.Y. Zhu, Electrochim. Acta 53 (2008) 7061.